J. Pineal Res. 2013
Doi:10.1111/jpi.12097

Journal of Pineal Research

Chronic melatonin treatment rescues electrophysiological and neuromorphological deficits in a mouse model of Down syndrome

Abstract: The Ts65Dn mouse (TS), the most commonly used model of Down syndrome (DS), exhibits several key phenotypic characteristics of this condition. In particular, these animals present hypocellularity in different areas of their CNS due to impaired neurogenesis and have alterations in synaptic plasticity that compromise their cognitive performance. In addition, increases in oxidative stress during adulthood contribute to the age-related progression of cognitive and neuronal deterioration. We have previously demonstrated that chronic melatonin treatment improves learning and memory and reduces cholinergic neurodegeneration in TS mice. However, the molecular and physiological mechanisms that mediate these beneficial cognitive effects are not yet fully understood. In this study, we analyzed the effects of chronic melatonin treatment on different mechanisms that have been proposed to underlie the cognitive impairments observed in TS mice: reduced neurogenesis, altered synaptic plasticity, enhanced synaptic inhibition and oxidative damage. Chronic melatonin treatment rescued both impaired adult neurogenesis and the decreased density of hippocampal granule cells in trisomic mice. In addition, melatonin administration reduced synaptic inhibition in TS mice by increasing the density and/or activity of glutamatergic synapses in the hippocampus. These effects were accompanied by a full recovery of hippocampal LTP in trisomic animals. Finally, melatonin treatment decreased the levels of lipid peroxidation in the hippocampus of TS mice. These results indicate that the cognitive-enhancing effects of melatonin in adult TS mice could be mediated by the normalization of their electrophysiological and neuromorphological abnormalities and suggest that melatonin represents an effective treatment in retarding the progression of DS neuropathology.

Andrea Corrales[1], Rebeca Vidal[1,2,3], Susana García[1], Verónica Vidal[1], Paula Martínez[1], Eva García[1], Jesús Flórez[1], Emilio J. Sanchez-Barceló[1], Carmen Martínez-Cué[1,*] and Noemí Rueda[1,*]

[1]Department of Physiology and Pharmacology, School of Medicine, University of Cantabria, Santander, Spain; [2]Institute of Biomedicine and Biotechnology (IBBITEC,UC-CSIC-IDICAN), Santander, Spain; [3]CIBERSAM Instituto de Salud Carlos III, Spain

Key words: Down syndrome, glutamatergic synapses, hippocampus, long-term potentiation, melatonin, neurogenesis, oxidative stress, Ts65Dn

Address reprint requests to Carmen Martínez-Cué and Noemí Rueda, Laboratory of Neurobiology of Learning, Department of Physiology and Pharmacology, Faculty of Medicine, University of Cantabria, C/Cardenal Herrera Oria s/n, 39011 Santander, Spain.
E-mails: martinec@unican.es and ruedan@unican.es
*These authors have contributed equally to this work.

Received August 12, 2013;
Accepted September 20, 2013.

Introduction

Ts65Dn mice (TS), the most commonly used model of Down syndrome (DS), exhibit numerous phenotypic characteristics of DS, including cognitive deficits due to impairments in hippocampal morphology and function [1]. These cognitive impairments appear in early life stages [2, 3] and become more pronounced during adulthood [4, 5].

One of the neuromorphological substrates of the cognitive deficits in TS mice and in DS individuals is the hypocellularity found in different areas of the central nervous system (CNS), including the hippocampus, presumably due to reduced neurogenesis. Altered pre- and postnatal neurogenesis has been demonstrated in individuals with DS and in TS mice and has been implicated in the cognitive deficits found in both conditions [1, 6]. Restoring neurogenesis by administering fluoxetine, lithium or the α5-selective negative allosteric modulator of the $GABA_A$ receptor RO4938581 restores cognitive abilities in the TS mouse model of DS [2, 7, 8]. Adult hippocampal neurogenesis has an important role in the establishment of hippocampal long-term potentiation (LTP) [9, 10], which is considered to be the electrophysiological substrate of learning and memory [11]. TS mice show a marked reduction in LTP in the CA1 and DG areas that correlates with their cognitive deficits [12–15].

One of the mechanisms proposed to underlie this altered synaptic plasticity in TS animals is enhanced inhibition due to an imbalance between excitatory and inhibitory neurotransmission. TS mice have increased GABA-mediated inhibition and a concomitant decrease in glutamatergic transmission resulting in impaired hippocampal LTP [12–16]. Different pharmacological manipulations that restore or improve the balance between excitatory and inhibitory transmission rescue neural plasticity and cognitive abilities in the TS mouse model of DS [7, 17–19].

Another mechanism that has been implicated in altering cognitive and neuronal function in DS is increased oxidative stress. In early life stages, DS individuals present enhanced oxidative stress including elevated levels of lipid peroxidation [20–24], which can modify processes such as neurogenesis, differentiation, migration, net connection and neuronal survival [23–25]. In later life stages, oxidative stress can also contribute to the age-related progression of cognitive and neuronal degeneration associated with DS

JPI | 12097 | WILEY | Dispatch: 4.11.13 | CE: Ashok
Journal Code | Manuscript No. | No. of pages: 11 | PE: Vigneswari

[26–28]. Both DS individuals and TS mice overexpress *SOD1*, the gene responsible for the formation of superoxide dismutase, an enzyme that modifies oxygen free radicals into hydrogen peroxide, leading to the overproduction of highly reactive oxygen free radicals. In addition, in DS, the overexpression of the *APP* gene leads to the overproduction of Aβ peptides and plays a pivotal role in the regulation of oxidative stress [28].

Melatonin is an indoleamine that has been consistently demonstrated to have neuroprotective effects [29–32]. Among the mechanisms underlying these effects are its free radical–scavenging and antioxidant properties [33, 34], its beneficial effect on neurogenesis [29, 30] and its ability to promote structural and functional neuroplasticity [30, 35–38]. Furthermore, it improves cognitive deficits in various mouse models of different neuropathologies [30, 31, 39]. These studies suggest that melatonin could be a useful tool to improve the functional and neuromorphological abnormalities of the DS brain.

In a previous study, we showed that chronic melatonin treatment improves spatial learning and memory and delays the degeneration of cholinergic neurons in adult TS mice [40]. The aim of the present study was to evaluate the mechanisms by which melatonin exerts its cognitive-enhancing effects in TS mice. Therefore, we have studied the effect of chronic treatment with this indoleamine on adult hippocampal neurogenesis, on synaptic plasticity, on excitatory/inhibitory balance and on brain lipid peroxidation in middle-aged TS mice.

Material and methods

Animals and housing

This study was approved by the Cantabria University Institutional Laboratory Animal Care and Use Committee and was carried out in accordance with the Declaration of Helsinki and the European Communities Council Directive (86/609/EEC). Mice were generated by repeated backcrossing of B6EiC3Sn a/A-Ts(17<16>)65Dn (TS) females with C57BL/6Ei x C3H/HeSNJ (B6EiCSn) F1 hybrid males. The parental mouse generation was provided by the Robertsonian Chromosome Resources (The Jackson Laboratory, Bar Harbor, ME, USA), and mating was performed in the University of Cantabria animal facilities. In all experiments, TS mice were compared to euploid littermates (CO). To determine the presence of the trisomy, animals were karyotyped using real-time quantitative PCR (qPCR) as previously described [41]. Because C3H/HeSnJ mice carry a recessive mutation that leads to retinal degeneration (RD), all animals were genotyped by standard PCR to identify and exclude mice carrying this gene. Mice were housed individually and maintained under a 12/12 hr light/dark cycle. Mice were allowed free access to rodent chow and water.

In this study, two cohorts of male mice were used. In the first cohort, eight animals per group (CO-vehicle; CO-Mel; TS-vehicle; TS-Mel) were used to perform the immunohistochemical studies (neurogenesis and inhibitory and excitatory synapse markers). The second cohort (CO-vehicle = 11; CO-Mel = 9; TS-vehicle = 9; TS-Mel = 9) was used to evaluate the effects of melatonin on LTP and brain oxidative stress.

Melatonin treatment

TS and CO male mice were treated with either melatonin (Mel) or its diluents (vehicle) and assigned to one of four experimental groups: TS-Mel, CO-Mel, TS-vehicle, and CO-vehicle. Melatonin (100 mg/L; Sigma-Aldrich, Madrid, Spain) was dissolved in absolute ethanol and then added to drinking water at a final ethanol concentration of 0.06%. Fresh melatonin solution was prepared twice a week in feeding bottles that were protected from light. The estimated daily melatonin intake for each mouse was 0.5 mg, based on an average daily water consumption rate of 5 mL/day. TS and CO mice in the vehicle groups received tap water containing 0.06% ethanol. Daily water consumption was similar for all experimental groups. All mice were 6–6.5 months old at the beginning of the treatment and between 11 and 11.5 months of age at the time of histological procedures. Those animals used for electrophysiology and the ELISA assay continued receiving treatment with melatonin or vehicle until they were 12 months-old.

Hippocampal LTP recording

Mice were decapitated, and the brains were rapidly removed. The hippocampi were dissected, and 400 μm slices were cut using a tissue chopper. Slices were allowed to recover for at least 1 hr in an interface chamber at room temperature in artificial cerebral spinal fluid (ACSF) containing (in mM) 120 NaCl, 3.5 KCl, 2.5 $CaCl_2$, 1.3 $MgSO_4$, 1.25 NaH_2PO_4, 26 $NaHCO_3$ and 10 D-glucose (saturated with 95% O_2 and 5% CO_2). Field excitatory postsynaptic potentials (fEPSPs) were recorded from the CA1 stratum radiatum with a glass micropipette (1–4 MΩ) containing 2 M NaCl and evoked by stimulation of the Schaffer collaterals using insulated bipolar platinum/iridium electrodes >500 μm away from the recording electrode. The stimulus strength was adjusted to evoke fEPSPs that were equal to 50% of the relative maximum amplitude, not including any superimposed population spike. After stable baseline recordings (100 μs pulse-duration, 0.033 Hz), LTP was induced by theta burst stimulation (TBS; 10 trains of 5 pulses at 100 Hz and intervals of 200 ms). The duration of the stimulation pulses was doubled during the tetanus. fEPSPs were amplified, band-pass-filtered (1 Hz-1 kHz) and stored in a computer using the Spike2 program (Spike2, Cambridge Electronic Design, Cambridge, UK). For analysis, fEPSP slopes were expressed as percentages of the baseline values recorded. Results from several slices were expressed as means $\pm$ S.E.M.

Immunohistochemistry

The animals used for histology and cell counting were deeply anesthetized with pentobarbital and transcardially perfused with saline followed by 4% paraformaldehyde. After being removed and postfixed in 4% paraformaldehyde

overnight at 4°C and transferred into 30% sucrose, the brains were frozen in dry ice and sliced coronally in a cryostat (50 μm thick sections). Series of brain slices were randomly made up of one section out of every nine for the immunohistochemistry protocol. A randomly chosen series was used to perform Nissl staining to calculate the subgranular zone (SGZ) total area of each mouse. The total SGZ extent was measured by the standard Cavalieri method ~~as described previously by Llorens-Martin et al. [42]~~ using a semiautomatic system (ImageJ v.1.33, NIH, USA, http://rsb.info.nih.gov/ij/).

Mature granule cell count

Mature granule cells in the hippocampal granule cell layer (GCL) were counted in series of one-in-nine sections stained with 4′6-diamidino-2-phenylindole (DAPI, Calbiochem, 1:1000) for 10 min in 0.1 M phosphate buffer (PB). Cell counts were performed using a previously described physical dissector system coupled with confocal microscopy [42]. Random numbers were generated to select the points at which to locate the dissectors. Six dissectors in each section were measured. At selected points, the confocal microscope (Leica SPE) was directed toward a position previously established randomly inside the GCL. Next, at each point, a series of confocal images was serially recorded, keeping to the general rules of the physical dissector and the unbiased stereology. The confocal images were then analyzed on a computer with the aid of the ImageJ software (ImageJ, v. 1.33, NIH, Bethesda, MD, USA, http://rsb.info.nih.gov/ij). Every successive pair of images was used, with one considered as the reference image and the other the sample image. Next, the sample image became the reference image for the next pair of images, and so on. The cells were counted with the NIH ImageJ Cell Counter, labeling each cell on the screen the first time it appears in the series of confocal images. The software generated the total number of cells when the dissector brick was completed. For counting the mature granule neurons in the GCL, the dissector frame was a square situated randomly inside the GCL. The number of cells was then divided by the reference volume of the dissector (this parameter is the volume of a cube formed by the area of the frame multiplied by the height of the dissector) to obtain the number of cells per volume unit (cell density).

Cell proliferation in the SGZ (Ki67 immunofluorescence)

Slices were initially pre-incubated in PB with Triton X-100 0.5% and bovine serum albumin (BSA) 0.1%, and then immunohistochemistry was performed as described previously [7]. Briefly, free-floating slices were incubated with primary antibodies (rabbit anti-Ki67, 1:750; Neo Markers, USA) diluted in PB with Triton X-100 0.5% and BSA 0.1% (PBTBSA) for 2 days at 4°C. Then, slices were incubated overnight at 4°C with secondary antibody (donkey anti-rabbit-Alexa Fluor 488, 1:1000, Molecular Probes, Eugene, OR, USA). The sections were counterstained with DAPI and mounted in gelatin-covered slides to be analyzed and photographed. The total number of Ki67-positive cells was counted in the selected sections with the help of an optical fluorescence microscope (Zeiss Axioskop 2 plus, 40× objective) using the optical dissector method previously described [43].

Neurodifferentiation (doublecortin/calretinin immunofluorescence)

One-in-nine series of 50 μm sections of mouse brains were used for the determination of cells expressing immature markers: doublecortin (DCX) and/or calretinin (CLR). Slices were initially preincubated in PBTBSA, and then dual immunohistochemistry was performed as described previously [42]. The primary antibodies used were goat anti-doublecortin (1:250; Santa Cruz, USA) and rabbit anti-calretinin (1:3000; Swant, Switzerland). The primary antibodies were recognized with an Alexa Fluor 594-conjugated donkey anti-goat and an Alexa Fluor 488-conjugated donkey anti-rabbit antibody (Alexa-conjugated antibodies from Molecular Probes, 1:1000). The sections were incubated with both primary antibodies at the same time and then with both secondary antibodies at the same time. The sections were then analyzed and photographed under a confocal microscope (Leica SP5). Quantification of DCX and CLR expression was performed according to stereological procedures of physical dissector previously described by Llorens-Martin et al. [42]. At each point of the section to be registered, we counted all the immature cells in the reference area using ImageJ. Next, the number was divided by the reference area of the side of the prism aligned with the SGZ to obtain the number of cells per area unit (the reference area for the side of the prism is the length of the side of the frame multiplied by the height of the dissector). The cell density was then multiplied by the SGZ area to obtain the total number of cells for each of the different populations of immature neurons. The number of immature neurons is presented as either DCX+/CLR− or total CLR+ (i.e. DCX+/CLR+ plus DCX−/CLR+).

Density of glutamatergic and GABAergic synapse markers (VGLUT1 and GAD65 immunofluorescence)

One-in-nine series of 50 μm sections of mouse brains were used for the determination of GABAergic and glutamatergic synapses. Slices were initially preincubated in PBTBSA, and then dual immunohistochemistry was performed as described previously [44]. Glutamatergic and GABAergic boutons in the molecular layer (ML) of the hippocampus were identified with anti-vesicular glutamate transporter 1 (VGLUT1, 1:2500; Chemicon, Temecula, CA, USA), a glutamatergic synapse marker, followed by Alexa Fluor 488-conjugated goat anti-guinea pig Ig (1:1000; Invitrogen, Carlsbad, CA, USA) and with anti-glutamic acid decarboxylase (GAD65, 1:250; Chemicon), a GABAergic synapse marker, followed by Alexa Fluor 594-conjugated donkey anti-mouse Ig (1:1000; Invitrogen).

Measurements were performed in images obtained with a confocal microscope (Leica SP5), using a 63× 1.4 NA objective and a 9× zoom. For each marker, four sections per animal were used comprising the entire hippocampus, and one random area in the hippocampus per section was

measured. Image analysis was performed with the aid of the NIH ImageJ software. Briefly, boutons with positive immunofluorescence (either VGLUT1 or GAD65 because these markers never colocalize) were measured separately applying the same threshold to all pictures. Images were first converted to grey scale to improve the contrast between signal and noise. Areas were measured inside a reference circle with a standard size of 325 μm^2. A reference space was located in the inner ML of the hippocampal DG, lining the most external layer of granule neurons in the GCL. The percentage of reference area occupied by VGLUT1- and GAD65- positive boutons was calculated.

Quantitation of lipid peroxidation in brain tissue

To quantify lipid peroxidation levels, 4-hydroxynonenal (HNE) Adduct ELISA Kit (OxiSelect™ HNE Adduct ELISA Kit, STA-338; Cell Biolabs, San Diego, CA, USA) was used to detect and measure hippocampal and cortex levels of HNE protein adducts in seven animals of each group. Briefly, tissue samples were homogenized in 1X PBS containing proteinase inhibitors (1:100, Protease Inhibitor Cocktail Set III, Merck, Darmstadt, Germany) and centrifuged at 12,000 g for 10 min. The supernatant fraction was collected and stored at −80°C. The protein concentration was determined with a Lowry protein assay, and samples were diluted to 10 μg/mL. To quantify HNE levels, supernatant fractions were analyzed using an HNE Adduct ELISA Kit following the manufacturer′s instructions. Analyses were always performed in duplicate. OD_{450} values were detected on a microplate reader (Multiskan EX; Thermo Electron Corporation, Vantaa, Finland). HNE levels were calculated according to the standard curve.

Statistical analysis

LTP data were analyzed by repeated-measures (RM)-ANOVAs ('time' × 'treatment' × 'genotype'). The remaining neuromorphological and ELISA data were analyzed using two-way ('genotype' × 'treatment') ANOVAs. The means of each experimental group were compared post-hoc by Student's *t*-test if two groups were compared or by Bonferroni tests if more than two groups were compared. All the analyses were performed using SPSS (version 21.0) for Windows. The *F* values of RM-ANOVAs, two-way ANOVAs, and post hoc analysis of each independent neuromorphological and electrophysiological variable tested are shown in Table 1.

Results

Figure 1(A) shows the immunocytochemical detection of mature granule neurons (DAPI+ cells) in the GCL of the DG of TS and CO mice treated with either melatonin or vehicle. The quantitative analysis of this cell population showed that vehicle-treated TS mice had a significantly lower density of DAPI+ cells than CO animals ($P = 0.03$). Melatonin increased the density of DAPI+ cells in both genotypes ($P = 0.003$; Table 1). After chronic treatment with melatonin, the density of granule neurons was significantly increased in the GCL of TS mice to levels similar to those observed in vehicle-treated CO mice (TS-melatonin versus CO-vehicle: $P = 0.25$; Fig. 1B). In CO mice, melatonin slightly increased the density of DAPI+ cells, although this effect did not reach statistical significance (CO-melatonin versus CO-vehicle: $P = 0.07$; Fig. 1B).

Cells undergoing different stages of adult hippocampal neurogenesis were identified and quantified using specific markers for proliferation and differentiation. To estimate the density of the actively dividing cells, we used Ki67 immunohistochemistry (Fig. 2B, up and second row). The density of Ki67+ cells in the SGZ was reduced in vehicle-treated TS mice compared to the vehicle-treated CO group ($P < 0.001$; Fig. 2C). Statistical analysis showed that melatonin treatment significantly increased the density of Ki67+ cells in TS mice compared to those of vehicle-treated TS mice (TS-vehicle versus TS-melatonin: $P = 0.01$; Table 1; Fig. 2C). By contrast, melatonin treatment did not modify the density of this cell population in CO mice.

Table 1. *F* values of RM-MANOVA, MANOVA (genotype x treatment) and post hoc analysis of each variable tested

	Genotype	Treatment	Genotype × Treatment
Inmunohistochemistry			
DAPI+ cells	$F_{1,29} = 4.99$; $P < 0.05$	$F_{1,29} = 11.00$; $P < 0.01$	$F_{1,29} = 0.05$; $P = 0.82$
Ki67+ cells	$F_{1,29} = 27.73$; $P < 0.001$	$F_{1,29} = 1.52$; $P = 0.22$	$F_{1,29} = 1.16$; $P = 0.29$
DCX+ cells	$F_{1,29} = 3.89$; $P = 0.059$	$F_{1,29} = 7.61$; $P < 0.01$	$F_{1,29} = 1.52$; $P = 0.22$
CLR+ cells	$F_{1,29} = 6.30$; $P < 0.05$	$F_{1,29} = 1.51$; $P = 0.22$	$F_{1,29} = 5.29$; $P < 0.05$
GABAergic boutons (GAD65)	$F_{1,29} = 137.95$; $P < 0.001$	$F_{1,29} = 0.04$; $P = 0.99$	$F_{1,29} = 1.02$; $P = 0.32$
Glutamatergic boutons (VGLUT)	$F_{1,29} = 28.49$; $P < 0.001$	$F_{1,29} = 13.57$; $P < 0.001$	$F_{1,29} = 4.46$; $P < 0.05$
Levels of HNE			
Cortex	$F_{1,25} = 9.64$; $P < 0.01$	$F_{1,25} = 6.91$; $P < 0.05$	$F_{1,25} = 2.20$; $P = 0.15$
Hippocampus	$F_{1,25} = 2.50$; $P = 0.12$	$F_{1,25} = 0.29$; $P = 0.59$	$F_{1,25} = 2.82$; $P = 0.10$
LTP results			
Basal	$F_{1,35} = 0.19$; $P = 0.65$	$F_{1,35} = 0.01$; $P = 0.91$	$F_{1,35} = 0.19$; $P = 0.65$
After theta burst stimulation	$F_{1,35} = 7.85$; $P < 0.01$	$F_{1,35} = 4.86$; $P < 0.05$	$F_{1,35} = 1.80$; $P = 0.18$
Post hoc comparisons between each pair of potentiation curves			
CO-Veh versus TS-Veh	$F_{1,17} = 11.09$; $P < 0.01$		
TS-Veh versus TS-mel		$F_{1,15} = 15.10$; $P < 0.001$	
CO-Veh versus CO-mel		$F_{1,17} = 0.25$; $P = 0.62$	
CO-Veh versus TS-mel			$F_{1,17} = 0.19$; $P = 0.66$

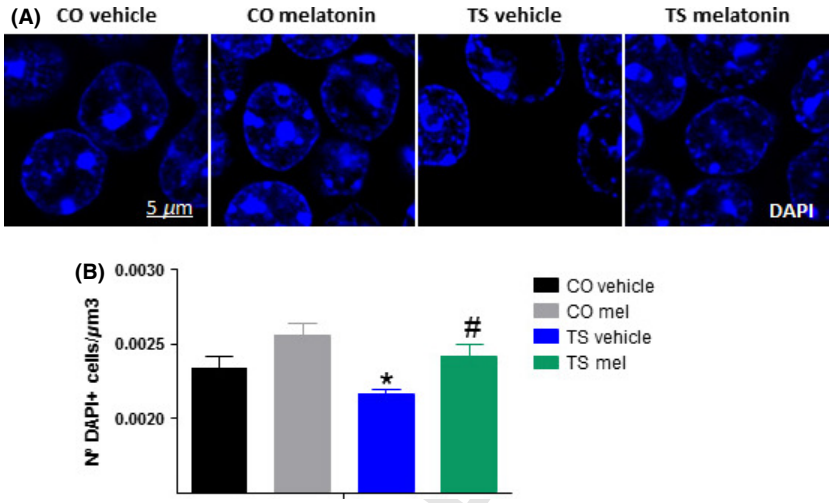

Fig. 1. (A) Representative images of DAPI in the DG region of hippocampus of vehicle- and melatonin-treated TS and CO mice. (B) Means ± S.E.M. of the density of mature granule neurons in the GCL of TS and of CO mice treated with melatonin or vehicle. *$P < 0.05$ TS versus CO; #$P < 0.05$ melatonin versus vehicle; Bonferroni post-hoc tests after significant MANOVAs.

We then performed dual immunohistochemistry using specific markers for the determination of proteins expressed by different subpopulations of hippocampal neurons in consecutive developmental stages in TS and CO mice treated with either melatonin or vehicle (Fig. 2A). For the determination of immature neurons, we performed immunohistochemistry for the early neuronal marker DCX in the different groups of mice (Fig. 2B, third row). Vehicle-treated TS animals showed a reduced density of DCX+ cells compared to CO animals ($P = 0.003$), and chronic melatonin treatment rescued this alteration in TS mice ($P = 0.01$; Fig 2C). Indeed, after chronic melatonin treatment, TS mice did not differ in the number of DCX+/CLR− cells from vehicle-treated CO mice (CO-vehicle versus TS-Mel: $P = 0.58$; Table 1; Fig. 2C).

Cells undergoing later differentiation stages were evaluated using the neuronal marker CLR (Fig. 2B, fourth row). The density of CLR+ cells (Fig. 2C; including both DCX+/CLR+ and DCX−/CLR+ phenotypes) was reduced in TS mice compared to vehicle-treated-CO mice ($P = 0.018$; CO-vehicle versus TS-vehicle: $P = 0.006$). However, the density of CLR+ cells was normalized after chronic melatonin treatment in TS mice (CO-vehicle versus TS-Mel: $P = 0.48$; Fig. 2C).

Figure 3 shows the levels of HNE in the cortices and hippocampi of TS and CO mice. Vehicle-treated TS mice had increased levels of lipid peroxidation in the cortex ($P = 0.005$) and in the hippocampus ($P = 0.015$; Table 1). Melatonin administration significantly reduced the levels of HNE in the cortex ($P = 0.015$) but not in the hippocampus ($P = 0.59$) of TS or CO animals. However, post hoc analysis revealed that the increase in HNE levels in the hippocampus of TS-vehicle mice compared to CO-vehicle mice was no longer significant after melatonin treatment ($P = 0.42$; Fig. 3).

To assess the effect of chronic melatonin treatment on hippocampal synaptic plasticity in TS and CO mice, we used a theta burst stimulus (TBS) to induce LTP in the Schaffer collaterals-CA1 region (SC-CA1) of the hippocampus. No significant differences were found in fEPSP amplitudes in the baselines of the four groups of mice ($P = 0.93$, Table 1; Fig. 4). Analysis of fEPSPs in vehicle-treated TS mice revealed deficits in TBS-induced LTP in CA1 with respect to vehicle-treated CO mice ($P = 0.004$; Fig. 4). Melatonin produced an enhancement of LTP in TS mice ($P = 0.001$). These findings indicate that chronic melatonin treatment completely rescued LTP in TS mice, as the mean fEPSP slopes did not differ between melatonin-treated TS mice and vehicle-treated CO mice ($P = 0.66$; Fig. 4). However, chronic melatonin administration did not modify LTP in CO animals ($P = 0.62$).

The analysis of the number of GABAergic (GAD65+) and glutamatergic (VGLUT1+) synaptic boutons in the hippocampal ML revealed that vehicle-treated TS mice showed reduced VGLUT1 immunoreactivity (Fig. 5A, upper row) and an increased area occupied by GAD65+ boutons compared to vehicle-treated CO mice (Fig. 5A, lower row; VGLUT1; $P < 0.001$; GAD65; $P < 0.001$).

Remarkably, melatonin treatment significantly increased the percentage of the area occupied by VGLUT1 boutons in TS mice, but no changes in the GABAergic synapse marker GAD65 were observed in this group of animals (VGLUT1: $P = 0.001$; GAD65: $P = 0.99$; Table 1). In CO animals, melatonin treatment did not modify the percentage of the area occupied by GABAergic or glutamatergic boutons (Fig. 5B).

Discussion

In this study, we investigated the putative mechanisms that mediate the cognitive-enhancing effects of chronic melatonin treatment in adult TS mice. In particular, we studied the effects of melatonin on the main electrophysiological and neuromorphological alterations that have been proposed to underlie learning and memory deficits in the TS mouse model of DS, i.e. reduced hippocampal cellularity, adult neurogenesis, altered synaptic plasticity due to enhanced inhibition and increased oxidative stress [1, 28, 45].

Reductions in neuronal number in different areas of the CNS appear to compromise cognitive function in DS and in the TS mouse. This hypocellularity is particularly important in the hippocampus due to its major impact on spatial learning and memory. As previously shown by

LOW RESOLUTION COLOR FIG

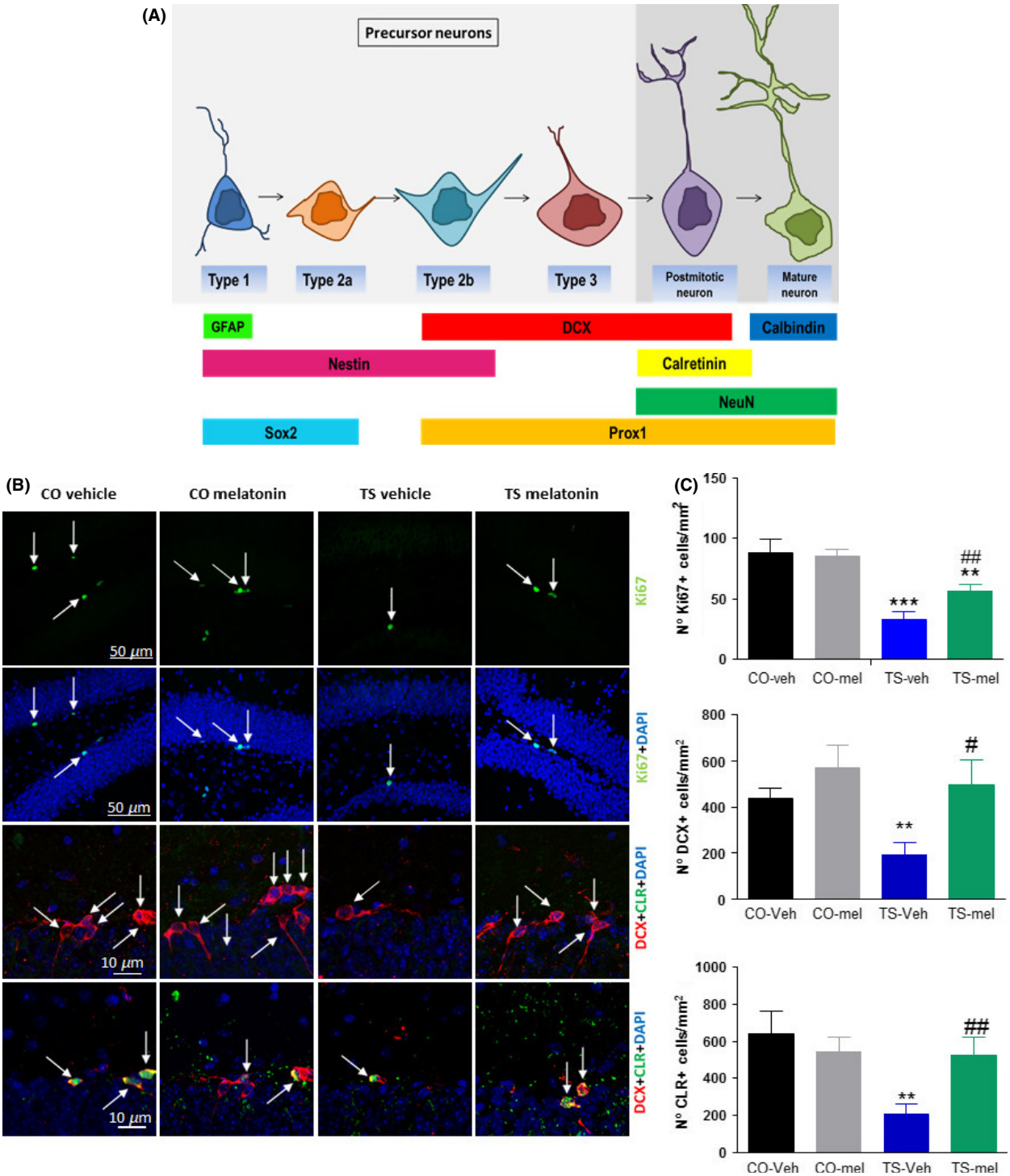

Fig. 2. (A) Time courses for the expression of specific molecular markers during different stages of adult DG neurogenesis. Modified from Contestabile et al. [8]. (B) Representative images of Ki67 (up row), coimmunostaining of Ki67 and DAPI (second row) and of immature neurons expressing DCX (third row) and CLR (fourth row) in the DG of TS and CO mice treated with vehicle or melatonin. (C) Means ± S.E.M. of the density of Ki67+ cells and of immature neurons DCX+/CLR− and CLR+ neurons in the SGZ of the hippocampus of vehicle- or melatonin- treated TS and CO mice. $^{**}P < 0.01$; $^{***}P < 0.001$ TS versus CO; $\#P < 0.05$, $\#\#P < 0.01$ melatonin versus vehicle; Bonferroni post-hoc tests after significant MANOVAs.

numerous studies [7, 43, 46], the density of mature granule neurons is reduced in the GCL of TS mice. This reduction may be due to increased cell death and/or to reduced proliferation in the SGZ. Interestingly, we found that melatonin treatment rescued the density of granule cells in TS mice.

Reduced neurogenesis is likely to be one of the mechanisms implicated in the impaired learning and memory

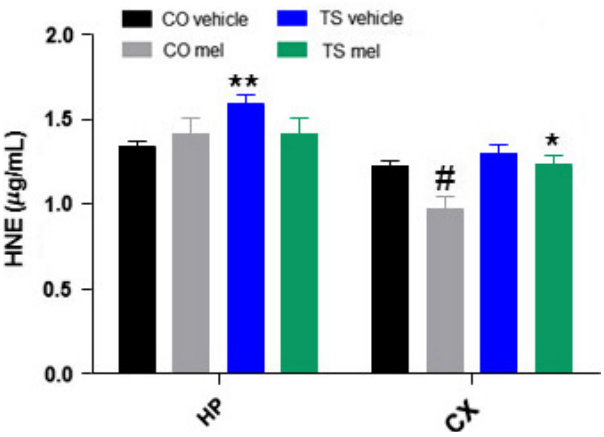

Fig. 3. Means ± S.E.M. of the HNE levels in the cortex and hippocampus of vehicle-or melatonin-treated TS and CO mice (n = 7 animals of each group). $*P < 0.05$; $**P < 0.01$ TS versus CO; $\#P < 0.05$ vehicle-treated versus melatonin-treated mice. Bonferroni post-hoc tests after significant MANOVAs.

found in TS mice. Numerous studies have demonstrated that adult hippocampal neurogenesis is important for normal spatial learning and memory. When newborn cells are removed genetically, animals display impaired capacity for learning and memory [10, 47]. Similarly, most of the treatments that impair adult hippocampal neurogenesis also disrupt spatial cognition [47, 48]. Indeed, a significant negative correlation has been observed between performance in the Morris water maze (MWM) and the number of newly generated cells derived from adult neurogenesis in the DG of TS mice and euploid littermates [1, 49].

To evaluate the effects of chronic melatonin treatment on adult hippocampal neurogenesis in TS mice, we analyzed different subpopulations of newborn cells (Ki67-positive cells) and of new neurons under different stages of differentiation (identified by DCX- and CLR-labeling). In accordance with the results of a number of studies [2, 43, 49–51], adult TS mice had a lower density of proliferating cells and decreases in both populations of immature neurons in the SGZ of the DG. This reduction in the density of proliferating and differentiating cells is likely to be responsible for the hypocellularity found in TS hippocampi.

Previous studies showed that exogenous melatonin administration rescued or attenuated the reduction of neurogenesis found during aging in normal mice [29, 37, 52] and in several models of different neuropathologies [31, 53–55]. Similarly, our data demonstrate that in adult TS mice, melatonin enhanced adult hippocampal neurogenesis by increasing the density of proliferating cells. However, melatonin did not completely restore the density of progenitors under proliferation (Ki67+ cells) in TS mice. In DS, AβPP contributes to impaired neurogenesis by influencing neural precursor cell proliferation [56]. In our previous work [40], melatonin did not reduce the increased levels of AβPP expression in the hippocampus of TS mice, which may contribute to the incomplete recovery of cell proliferation in these animals. In addition, cell cycle disruptions and decreased cell proliferation beginning at early developmental stages in the TS mouse model of DS [2, 46, 57]. Thus, it is also possible that because the melatonin treatment regimen in the present study started at 6 months of age, the hypocellularity established in early developmental stages was not affected by this indoleamine treatment. Further studies will be necessary to clarify whether early melatonin administration may exert larger beneficial effects on cell proliferation in TS mice.

Melatonin completely rescued the density of immature neurons undergoing different stages of differentiation by normalizing the density of cells in intermediate DCX- and CLR-expressing stages. In agreement with this result, in vitro and in vivo studies have demonstrated that melatonin predominantly facilitates the transformation of precursor cells into mature neurons in the SVZ and SGZ of the adult mice [29, 58].

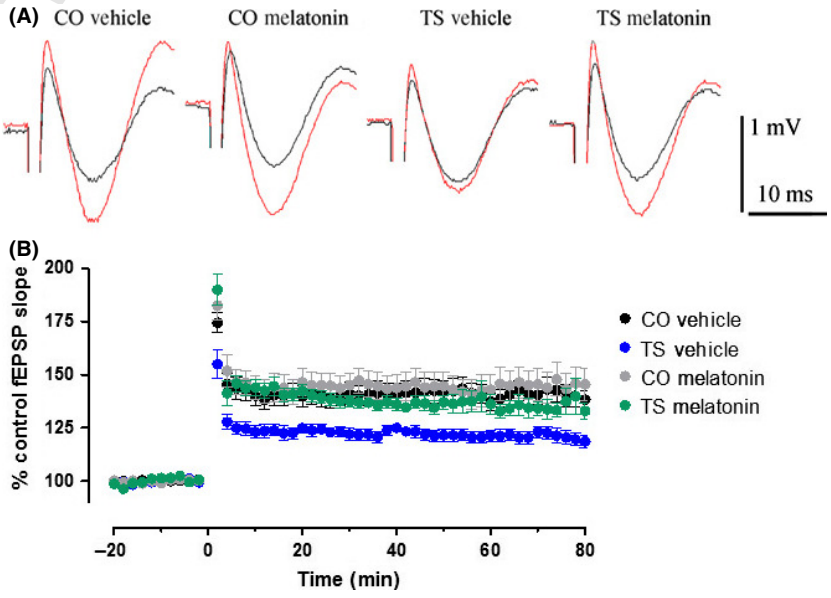

Fig. 4. (A) Representative fEPSPs traces recorded before issuing the stimulus (black) and at 60 min after stimulation (red) for each experimental group. Scale bars are 1 mV and 10 ms. (B) Means ± S.E.M. of fEPSPs (expressed as % versus basal) values from vehicle-treated CO (n = 11 slices from 11 different mice), vehicle-treated TS (n = 9 slices from 9 different mice), melatonin-treated CO (n = 9 slices from 9 different mice) and melatonin-treated TS (n = 9 slices from 9 different mice), respectively.

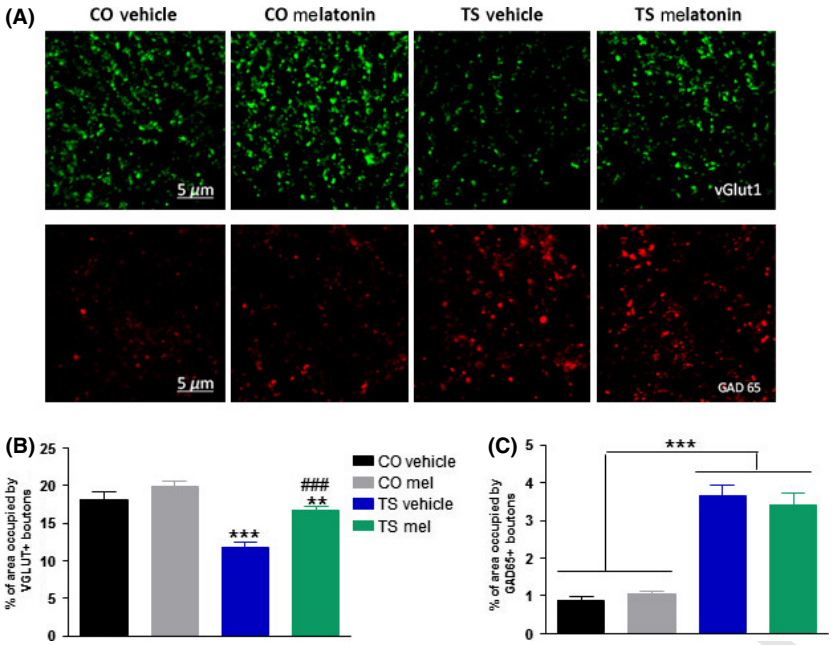

16 *Fig. 5.* (A) Representative confocal microscope images of boutons immunopositive for VGlut1 (green, glutamate synapses; up row) and GAD65 (red, GABAergic synapses; down row) in the inner ML of the hippocampal DG, lining the most external layer of granule neuron in the GCL of the four groups of animals. Means ± S.E.M. of the percentage of total immunopositive surface occupied by VGlut1 (B) and GAD65 (C) boutons of vehicle- and melatonin-treated TS and CO mice. $^{**}P < 0.01$; $^{***}P < 0.001$ TS versus CO; $\#\#\#P < 0.001$ melatonin vs. vehicle; Bonferroni post-hoc tests after significant MANOVAs.

Increase cell death is another putative mechanism implicated in the hippocampus hypocellularity and the altered cognitive abilities found in TS mice. Indeed, melatonin has been shown to induce neuroprotection due to its anti-apoptotic action through the prevention of the activation of the mitochondrial pathway [59].However, previous studies showed that apoptotic cell death during development or in adulthood is not involved in the reduced number of neurons found in the TS brain [60, 61]. Therefore, it is more likely that melatonin rescues the density of mature granule neurons in the hippocampus by increasing adult neurogenesis and survival.

Both DS individuals and TS mice present enhanced oxidative stress leading to premature neuronal death and cognitive dysfunction [22, 23, 62]. Consistent with previous results [22, 62], the levels of HNE, a specific marker of lipid peroxidation, were significantly increased in the hippocampus of vehicle-treated TS mice compared to CO mice. By contrast, TS mice did not show higher levels of HNE in cortex, suggesting that this region may exhibit more tolerance against oxidative stress than the hippocampus.

Melatonin rescued the levels of HNE in the hippocampus of TS mice; thus, its cognitive-enhancing effects in trisomic animals could also be partially due to its well-known antioxidant properties [33, 39, 63]. Although the antioxidant SGS-111, an analogue of the nootropic piracetam, administered from conception failed to improve learning and memory in the TS mouse model of DS [64], other antioxidants, such as vitamin E, delay impairment in cognitive performance, preserve markers of cholinergic cell survival, sustain hippocampal morphology and normalize oxidative stress in adult TS mice [62]. The free radical scavenging ability of melatonin is twice that of vitamin E [65], and melatonin is particularly effective in crossing the blood-barrier [66]. Thus, the reduction in lipid peroxidation in the hippocampus of TS mice after melatonin treatment might be implicated in the increase in granule cell density and the decrease in age-associated cognitive decline observed in these animals.

Numerous studies have demonstrated that TS mice present altered hippocampal synaptic plasticity that correlates with their cognitive alterations. In agreement with previous evidence [13–15], the present study showed that LTP was reduced in TS mice, and melatonin treatment for 5–6 months completely rescued LTP in the CA1 area in trisomic animals. Consistent with these findings, chronic melatonin treatment has been shown to rescue deficits in hippocampal LTP and spatial memory after intra-hippocampal injection of Aβ [30], although the acute application of melatonin directly to mouse and rat hippocampal slices inhibits LTP in the CA1 region [67–69].

Increasing evidence indicates that impaired LTP and the associated cognitive dysfunction in TS animals are mediated by a dysregulation between excitatory and inhibitory neurotransmission [15, 16, 19]. Consistent with previous results [7, 51], TS mice presented a reduced density of glutamatergic (VGLUT1-positive boutons) and an increased density of GABAergic (GAD65-positive boutons) synapse markers in the hippocampal ML indicating enhanced inhibition. Chronic melatonin administration to adult TS mice increased the density of glutamatergic synapse markers, thereby reducing inhibition. By contrast, this treatment did not have any effect on the area occupied by GAD65-positive boutons. Reducing synaptic inhibition by administering different antagonists and negative allosteric modulators of the $GABA_A$ receptor has been proven to rescue synaptic plasticity, neuromorphological and cognitive alterations in the TS mouse model of DS [7, 17, 18]. In addition, LTP in the SC-CA1 pathway is known to be dependent upon the activation of NMDA receptors. Recently, a high-affinity selective $GABA_B$ antagonist improved LTP in TS mice by increasing the NMDA receptor-mediated component [19]. Melatonin also protects and

increases NMDA receptor subunits 2A and 2B concentrations in rat hippocampus [70, 71]. Thus, at the postsynaptic level, the enhanced activation of NMDA receptors represents a possible mechanism by which melatonin could increase LTP in TS mice. Melatonin administration to TS mice might also restore LTP by increasing the density and/or activity of glutamatergic synapses. In addition, the restoration of the density of granule cells could improve afferent synaptic input from the DG and enhance the efficiency of excitatory signaling through the trisynaptic circuit, thereby enhancing LTP.

In young TS mice, several pharmacotherapies, including several selective GABAA receptor antagonists, the selective GABAA $\alpha5$ negative allosteric modulator RO4938581, lithium, fluoxetine and the long-acting $\beta2$ adrenergic agonist formoterol, have been shown to improve or normalize their cognitive performance, concomitantly to their neuromorphological and electrophysiological deficits [7, 8, 19, 72, 73]. In aged TS animals, like the ones used in this study, several drugs including the uncompetitive NMDA receptor antagonist memantine, the antioxidant vitamin E and the anti-inflammatory drug minocycline have also been reported to reduce the cognitive deterioration of these mice, and some age-related neuropathological hallmarks of DS [51, 62, 74]. However, none of these treatments have been proven to completely rescue the neuromorphorphological and electrophysiological deficits proposed to underlie DS-cognitive alterations as demonstrated in this work after chronic melatonin treatment. In addition, melatonin is normally well tolerated in adults, does not induce important side-effects and has been approved for human use; therefore, this indoleamine is a promising preventive therapy to slow the age-related progression of DS cognitive alterations.

In summary, melatonin administration to adult TS mice significantly increased the density of proliferating cells, the density of differentiating neuroblasts, and the density of mature granule cells while reducing the levels of lipid peroxidation. Furthermore, it reduced synaptic inhibition in the hippocampus of TS animals, leading to a complete recovery of LTP. Therefore, the normalization of the function and/or morphology of the hippocampus is likely to account for the cognitive-enhancing effects of chronic melatonin treatment previously demonstrated in TS mice. Our results provide evidence supporting the use of melatonin in clinical trials to alleviate cognitive deficits in the DS population prior to advanced memory decline. Regarding its efficacy as a preventive therapy in adults with DS, the initial dose, derived from this study to be administered to humans could be calculated according to the body surface area (BSA) normalization method previously described by Reagan-Shaw et al. [75].

Acknowledgements

This work was supported through grants from the Instituto de Formación e Investigación Marqués de Valdecilla (FMV-API 10/19), the Jerome Lejeune Foundation and the Spanish Ministry of Economy and Competitiveness (PSI2012-33652).

Author contributions

A.C. performed pharmacological treatments and histological studies. A.C. and R.V performed electrophysiological studies. P. M., S. G. and V.V. karyotyped the animals. E.G. performed ELISA studies. J. F. and E.S.-B. designed and discussed experiments. C.M.-C. and N.R. conceived the project, designed, supervised, conducted and interpreted experiments, analyzed the data and wrote the manuscript.

References

1. Rueda N, Flórez J, Martínez-Cué C. Mouse models of down syndrome as a tool to unravel the causes of mental disabilities. Neural Plast 2012; **2012**:584071.
2. Bianchi P, Ciani E, Guidi S et al. Early pharmacotherapy restores neurogenesis and cognitive performance in the Ts65Dn mouse model for Down syndrome. J Neurosci 2010; **30**:8769–8779.
3. Guidi S, Ciani E, Bonasoni P et al. Widespread proliferation impairment and hypocellularity in the cerebellum of fetuses with down syndrome. Brain Pathol 2011; **21**:361–673.
4. Granholm A-CH, Sanders LA, Crnic LS. Loss of cholinergic phenotype in basal forebrain coincides with cognitive decline in a mouse model of Down's syndrome. Exp Neurol 2000; **161**:647–663.
5. Hyde LA, Crnic LS. Age-related deficits in context discrimination learning in Ts65Dn mice that model Down syndrome and Alzheimer's disease. Behav Neurosci 2001; **115**:1239–1246.
6. Bartesaghi R, Guidi S, Ciani E. Is it possible to improve neurodevelopmental abnormalities in Down syndrome? Rev Neurosci 2011; **22**:419–455.
7. Martínez-Cué C, Martínez P, Rueda N et al. Reducing GABAA $\alpha5$ receptor-mediated inhibition rescues functional and neuromorphological deficits in a mouse model of Down syndrome. J Neurosci 2013; **33**:3953–3966.
8. Contestabile A, Greco B, Ghezzi D et al. Lithium rescues synaptic plasticity and memory in Down syndrome mice. J Clin Invest 2013; **123**:348–361.
9. Malberg JE, Eisch AJ, Nestler EJ et al. Chronic antidepressant treatment increases neurogenesis in adult rat hippocampus. J Neurosci 2000; **20**:9104–9110.
10. Imayoshi I, Sakamoto M, Ohtsuka T et al. Roles of continuous neurogenesis in the structural and functional integrity of the adult forebrain. Nat Neurosci 2008; **11**:1153–1161.
11. Cooke SF, Bliss TV. Plasticity in the human central nervous system. Brain 2006; **129**:1659–1673.
12. Siarey RJ, Carlson EJ, Epstein CJ et al. Increased synaptic depression in the Ts65Dn mouse, a model for mental retardation in Down syndrome. Neuropharmacology 1999; **38**:1917–1920.
13. Siarey RJ, Kline-Burgess A, Cho M et al. Altered signaling pathways underlying abnormal hippocampal synaptic plasticity in the Ts65Dn mouse model of Down syndrome. J Neurochem 2006; **98**:1266–1277.
14. Costa AC, Grybko MJ. Deficits in hippocampal CA1 LTP induced by TBS but not HFS in the Ts65Dn mouse: a model of Down syndrome. Neurosci Lett 2005; **382**:317–322.
15. Kleschevnikov AM, Belichenko PV, Villar AJ et al. Hippocampal long-term potentiation suppressed by increased

inhibition in the Ts65Dn mouse, a genetic model of Down syndrome. J Neurosci 2004; **24**:8153–8160.
16. Belichenko PV, Kleschevnikov AM, Masliah E et al. Excitatory-inhibitory relationship in the fascia dentata in the Ts65Dn mouse model of Down syndrome. J Comp Neurol 2009; **512**:453–466.
17. Rueda N, Florez J, Martinez-Cue C. Chronic pentylenetetrazole but not donepezil treatment rescues spatial cognition in Ts65Dn mice, a model for Down syndrome. Neurosci Lett 2008; **433**:22–27.
18. Braudeau J, Delatour B, Duchon A et al. Specific targeting of the GABA-A receptor α5 subtype by a selective inverse agonist restores cognitive deficits in Down syndrome mice. J Psychopharmacol 2011; **25**:1030–1042.
19. Kleschevnikov AM, Belichenko PV, Faizi M et al. Deficits in cognition and synaptic plasticity in a mouse model of Down syndrome ameliorated by GABAB receptor antagonists. J Neurosci 2012; **32**:9217–9227.
20. Perluigi M, du Domenico F, Fiorini A et al. Oxidative stress occurs early in Down síndrome pregnancy: a redox proteomics analysis of amniotic fluid. Proteomics Clin Appl 2011; **5**:167–168.
21. Pallardó FV, Degan P, D'ischia M et al. Multiple evidence for an early age pro-oxidant state in Down Syndrome patients. Biogerontology 2006; **7**:211–220.
22. Shichiri M, Yoshida Y, Ishida N et al. alpha-Tocopherol suppreses lipid peroxiation and behavioural and cognitive impairments in the Ts65Dn mouse model of Down syndrome. Free Radic Biol Med 2011; **15**:1801–1811.
23. Busciglio J, Yankner BA. Apoptosis and increased generation of reactive oxygen species in Down's syndrome neurons in vitro. Nature 1995; **378**:776–779.
24. Capone G, Kim P, Jovanovich S et al. Evidence for increased mitochondrial superoxide production in Down syndrome. Life Sci 2002; **70**:2885–2895.
25. Pelsman A, Hoyo-Vadillo C, Gudasheva TA et al. GVS-111 prevents oxidative damage and apoptosis in normal and Down's syndrome human cortical neurons. Int J Dev Neurosci 2003; **21**:117–124.
26. de Haan JB, Wolvetang EJ, Cristiano F et al. Reactive oxygen species and their contribution to pathology in Down syndrome. Adv Pharmacol 1997; **38**:379–402.
27. Busciglio J, Pelsman A, Helguera P et al. NAP and ADNF-9 protect normal and Down's syndrome cortical neurons from oxidative damage and apoptosis. Curr Pharm Des 2007; **13**:1091–1098.
28. Perluigi M, Butterfield DA. Oxidative stress and Down syndrome: a route toward Alzheimer-like dementia. Curr Gerontol Geriatr Res 2012; **2012**:724904.
29. Ramirez-Rodriguez F, Klempin F, Babu H et al. Melatonin modulates cell survival of new neurons in the hippocampus of adult mice. Neuropsychopharmacology 2009; **34**:2180–2191.
30. Liu XJ, Yuan L, Yang D et al. Melatonin protects against amyloid-β-induced impairments of hippocampal LTP and spatial learning in rats. Synapse 2013; **67**:626–636.
31. Yoo DY, Kim W, Lee CH et al. Melatonin improves D-galactose-induced aging effects on behavior, neurogenesis, and lipid peroxidation in the mouse dentate gyrus via increasing pCREB expression. J Pineal Res 2012; **52**:21–28.
32. Reiter RJ, Benitez-King G. Melatonin reduces neuronal loss and cytoskeletal deterioration: implications for psychiatry. Salud Mental 2009; **32**:3–11.
33. Galano A, Tan DX, Reiter RJ. Melatonin as a natural ally against oxidative stress: a physicochemical examination. J Pineal Res 2011; **51**:1–16.
34. Galano A, Tan DX, Reiter RJ. On the free radical scavenging activities of melatonin's metabolites, AFMK and AMK. J Pineal Res 2013; **54**:245–257.
35. Pascual R, Bustamante C. Structural neuroplastiticy induced by melatonin in entorhinal neurons of rats exposed to toluene inhalation. Acta Neurobiol Exp 2001; **71**:541–547.
36. Domínguez-Alonso A, Ramírez-Rodriguex G, Benítez-King G. Melatonin increases dendritogenesis in the hilus of hippocampal organotypic cultures. J Pineal Res 2012; **52**:427–436.
37. Ramirez-Rodriguez G, Ortiz-Lopez I, Dominguez-Alonso A et al. Chronic treatment with melatonin stimulates dendrite maturation and complexity in adult hippocampal neurogenesis of mice. J Pineal Res 2011; **50**:29–37.
38. Chen HY, Hung YC, Chen TY et al. Melatonin improves presynaptic protein SNAP-25, expression and dendritic spine density and enhances functional and electrophysological recovery following transient focal cerebral ischemia in rats. J Pineal Res 2009; **47**:313–317.
39. Olcese JM, Chao C, Mori T et al. Protection against cognitve deficits and markers of neurodegeneration by long-term oral administration of melatonin in a transgenic model of Alzheimer disease. J Pineal Res 2009; **47**:82–96.
40. Corrales A, Martínez P, García S et al. Long-term oral administration of melatonin improves spatial learning and memory and protects against cholinergic degeneration in middle-aged Ts65Dn mice, a model of Down syndrome. J Pineal Res 2013; **54**:346–358.
41. Liu DP, Schmidt C, Billings T et al. Quantitative PCR genotyping assay for the Ts65Dn mouse model of Down syndrome. Biotechniques 2003; **35**:1170–1174.
42. Llorens-Martín M, Torres-Alemán I, Trejo JL. Pronounced individual variation in the response to the stimulatory action of exercise on immature hippocampal neurons. Hippocampus 2006; **16**:480–490.
43. Llorens-Martín MV, Rueda N, Tejeda GS et al. Effects of voluntary physical exercise on adult hippocampal neurogenesis and behavior of Ts65Dn mice, a model of Down syndrome. Neuroscience 2010; **171**:1228–1240.
44. Trejo JL, Piriz J, Llorens-Martin MV et al. Central actions of liver-derived insulin-like growth factor I underlying its pro-cognitive effects. Mol Psychiatry 2007; **12**:1118–1128.
45. Cramer N, Galdzicki Z. From abnormal hippocampal synaptic plasticity in down syndrome mouse models to cognitive disability in down syndrome. Neural Plast 2012; **2012**:101542.
46. Contestabile A, Fila T, Ceccarelli C et al. Cell cycle alteration and decreased cell proliferation in the hippocampal dentate gyrus and in the neocortical germinal matrix of fetuses with Down syndrome and in Ts65Dn mice. Hippocampus 2007; **17**:665–678.
47. Dupret D, Revest JM, Koehl M et al. Spatial relational memory requires hippocampal adult neurogenesis. PLoS ONE 2008; **3**:e1959.
48. Deng W, Saxe MD, Gallina IS et al. Adult-born hippocampal dentate granule cells undergoing maturation modulate learning and memory in the brain. J Neurosci 2009; **29**:13532–13542.
49. Velazquez R, Ash JA, Powers BE et al. Maternal choline supplementation improves spatial learning and adult

hippocampal neurogenesis in the Ts65Dn mouse model of Down syndrome. Neurobiol Dis 2013; **58**:92–101.

50. Rueda N, Mostany R, Pazos A et al. Cell proliferation is reduced in the dentate gyrus of aged but not young Ts65Dn mice, a model of Down syndrome. Neurosci Lett 2005; **380**:197–201.
51. Rueda N, Llorens-Martin M, Florez J et al. Memantine normalizes several phenotypic features in the Ts65Dn mouse model of Down syndrome. J Alzheimers Dis 2010; **21**:277–290.
52. Ramírez-Rodríguez G, Vega-Rivera NM, Benítez-King G et al. Melatonin supplementation delays the decline of adult hippocampal neurogenesis during normal aging of mice. Neurosci Lett 2012; **530**:53–58.
53. Rennie K, de Butte M, Pappas BA. Melatonin promotes neurogenesis in dentate gyrus in the pinealectomized rat. J Pineal Res 2009; **47**:313–317.
54. Manda K, Ueno M, Anzai K. Cranial irradiation-induced inhibition of neurogenesis in hippocampal dentate gyrus of adult mice: attenuation by melatonin pretreatment. J Pineal Res 2009; **46**:71–78.
55. Crupi R, Mazzon E, Marino A et al. Melatonin's stimulatory effect on adult hippocampal neurogenesis in mice persists after ovariectomy. J Pineal Res 2011; **51**:353–360.
56. Trazzi S, Fuchs C, Valli E et al. The amyloid precursor protein (APP) triplicated gene impairs neuronal precursor differentiation and neurite development through two different domains in the Ts65Dn mouse model for Down syndrome. J Biol Chem 2013; **288**:20817–20829.
57. Lorenzi HA, Reeves RH. Hippocampal hypocellularity in the Ts65Dn mouse originates early in development. Brain Res 2006; **1104**:153–159.
58. Sotthibundhu A, Phansuwan-Pujito P, Govitrapong P. Melatonin increases proliferation of cultured neural stem cells obtained from adult mouse subventricular zone. J Pineal Res 2010; **49**:291–300.
59. Wang X. The antiapoptotic activity of melatonin in neurodegenerative diseases. CNS Neurosci Ther 2009; **15**:345–357.
60. Rueda N, Flórez J, Matínez-Cué C. The Ts65Dn mouse model of Down syndrome shows reduced expression of the Bcl-X(L) antiapoptotic protein in the hippocampus not accompanied by changes in molecular or cellular markers of cell death. Int J Dev Neurosci 2011; **29**:711–716.
61. Rueda N, Flórez J, Martínez-Cué C. Apoptosis in Down's syndrome: lessons from studies of human and mouse models. Apoptosis 2012; **2**:121–134.
62. Lockrow J, Prakasam A, Huang P et al. Cholinergic degeneration and memory loss delayed by vitamin E in a Down syndrome mouse model. Exp Neurol 2009; **216**:278–289.
63. Reiter RJ. Antioxidant actions of melatonin. Adv Pharmacol 1997; **38**:103–117.
64. Rueda N, Florez J, Martinez-Cue C. Effects of chronic administration of SGS-111 during adulthood and during the pre- and post-natal periods on the cognitive deficits of Ts65Dn mice, a model of Down syndrome. Behav Brain Res 2008; **188**:355–367.
65. Pieri C, Marra M, Moroni F et al. Melatonin: a peroxyl radical scavenger more effective than vitamin E. Life Sci 1994; **55**:271–276.
66. Chen YC, Sheen JM, Tain YL et al. Alterations in NADPH oxidase expression and blood-brain barrier in bile duct ligation-treated young rats: effects of melatonin. Neurochem Int 2012; **60**:751–758.
67. Ozcan M, Yilmaz B, Carpenter DO. Effects of melatonin on synaptic transmission and long-term potentiation in two areas of mouse hippocampus. Brain Res 2006; **1111**:90–94.
68. Sutcu R, Yonden Z, Yilmaz A et al. Melatonin increases NMDA receptor subunits 2A and 2B concentrations in rat hippocampus. Mol Cell Biochem 2006; **283**:101–105.
69. Takahashi Y, Okada T. Involvement of the nitric oxide cascade in melatonin-induced inhibition of long-term potentiation at hippocampal CA1 synapses. Neurosci Res 2011; **69**:1–7.
70. Talaei SA, Sheibani V, Salami M. Light deprivation improves melatonin related suppression of hippocampal plasticity. Hippocampus 2010; **20**:447–455.
71. Delibas N, Altuntas I, Yonden Z et al. Ochratoxin A reduces NMDA receptor subunits 2A and 2B concentrations in rat hippocampus: partial protective effect of melatonin. Hum Exp Toxicol 2003; **22**:335–339.
72. Dang V, Medina B, Das D et al. Formoterol, a long-acting β2 adrenergic agonist, improves cognitive function and promotes dendritic complexity in a mouse model of Down syndrome. Biol Psychiatry 2013; **???**/??–???. Doi: 10.1016/j.biopsych.2013.05.024. 11
73. Stagni F, Magistretti J, Guidi S et al. Pharmacotherapy with fluoxetine restores functional connectivity from the dentate gyrus to field CA3 in the Ts65Dn mouse model of Down syndrome. PLoS ONE 2013; **8**:e61689.
74. Hunter CL, Bachman D, Granholm AC. Minocycline prevents cholinergic loss in a mouse model of Down's syndrome. Ann Neurol 2004; **56**:675–688.
75. Reagan-Shaw S, Nihal M, Ahmad N. Dose translation from animal to human studies revisited. FASEB J 2008; **22**:659–661.

Author Query Form

Journal: JPI
Article: 12097

Dear Author,
During the copy-editing of your paper, the following queries arose. Please respond to these by marking up your proofs with the necessary changes/additions. Please write your answers on the query sheet if there is insufficient space on the page proofs. Please write clearly and follow the conventions shown on the attached corrections sheet. If returning the proof by fax do not write too close to the paper's edge. Please remember that illegible mark-ups may delay publication.
Many thanks for your assistance.

Query reference	Query	Remarks
1	**AUTHOR: Please provide the city name for 3rd afffiliation.**	
2	**AUTHOR: 'Llorens-Martin et al. [42]' found to be mismatch with this reference citation, please check.**	
3	**AUTHOR: Please check all website addresses and confirm that they are correct. (Please note that it is the responsibility of the author(s) to ensure that all URLs given in this article are correct and useable.)**	
4	**AUTHOR: Please give manufacturer information for "Leica SPE": company name, town, state (if USA), and country.**	
5	**AUTHOR: Please provide the city name for 'Neo Markers, UK'.**	
6	**AUTHOR: Please give manufacturer information for 'Zeiss Axioskop 2 plus': company name, town, state (if USA), and country.**	
7	**AUTHOR: Please provide the city and state name for 'Santa Cruz, USA'.**	
8	**AUTHOR: Please provide the city name for 'Swant, Switzerland'.**	
9	**AUTHOR: Please give manufacturer information for 'Leica SP5': company name, town, state (if USA), and country.**	
10	**AUTHOR: Please give manufacturer information for 'SPSS (version 21.0)': company name, town, state (if USA), and country.**	
11	**AUTHOR: Please provide the volume number, page range for reference [72].**	
12	**AUTHOR: Figure 1 has been saved at a low resolution of 128 dpi. Please resupply at 600 dpi. Check required artwork specifications at http://authorservices.wiley.com/bauthor/illustration.asp**	
13	**AUTHOR: Figure 2 has been saved at a low resolution of 136 dpi. Please resupply at 600 dpi. Check required artwork specifications at http://authorservices.wiley.com/bauthor/illustration.asp**	
14	**AUTHOR: Figure 3 has been saved at a low resolution of 108 dpi. Please resupply at 600 dpi. Check required artwork specifications at http://authorservices.wiley.com/bauthor/illustration.asp**	
15	**AUTHOR: Figure 4 has been saved at a low resolution of 154 dpi. Please resupply at 600 dpi. Check required artwork specifications at http://authorservices.wiley.com/bauthor/illustration.asp**	
16	**AUTHOR: Figure 5 has been saved at a low resolution of 144 dpi. Please resupply at 600 dpi. Check required artwork specifications at http://authorservices.wiley.com/bauthor/illustration.asp**	

WILEY-BLACKWELL

USING e-ANNOTATION TOOLS FOR ELECTRONIC PROOF CORRECTION

Required software to e-Annotate PDFs: Adobe Acrobat Professional or Adobe Reader (version 8.0 or above). (Note that this document uses screenshots from Adobe Reader X)
The latest version of Acrobat Reader can be downloaded for free at: http://get.adobe.com/reader/

Once you have Acrobat Reader open on your computer, click on the Comment tab at the right of the toolbar:

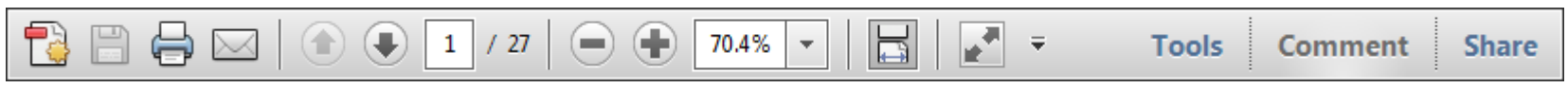

This will open up a panel down the right side of the document. The majority of tools you will use for annotating your proof will be in the Annotations section, pictured opposite. We've picked out some of these tools below:

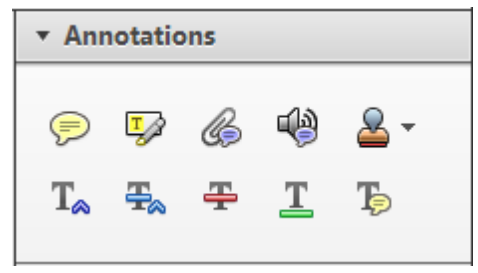

1. Replace (Ins) Tool – for replacing text.

Strikes a line through text and opens up a text box where replacement text can be entered.

How to use it

- Highlight a word or sentence.
- Click on the Replace (Ins) icon in the Annotations section.
- Type the replacement text into the blue box that appears.

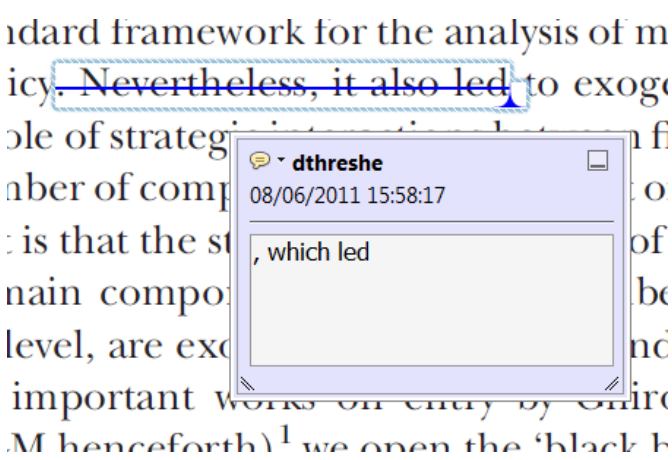

2. Strikethrough (Del) Tool – for deleting text.

Strikes a red line through text that is to be deleted.

How to use it

- Highlight a word or sentence.
- Click on the Strikethrough (Del) icon in the Annotations section.

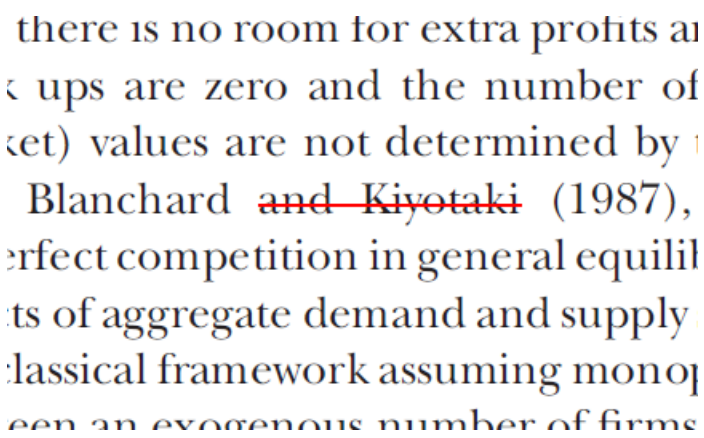

3. Add note to text Tool – for highlighting a section to be changed to bold or italic.

Highlights text in yellow and opens up a text box where comments can be entered.

How to use it

- Highlight the relevant section of text.
- Click on the Add note to text icon in the Annotations section.
- Type instruction on what should be changed regarding the text into the yellow box that appears.

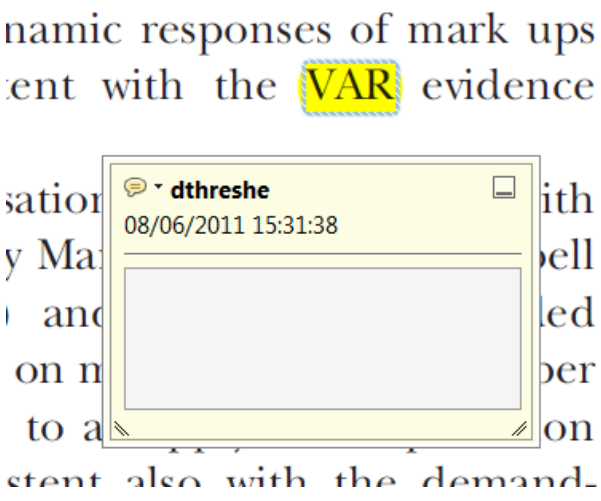

4. Add sticky note Tool – for making notes at specific points in the text.

Marks a point in the proof where a comment needs to be highlighted.

How to use it

- Click on the Add sticky note icon in the Annotations section.
- Click at the point in the proof where the comment should be inserted.
- Type the comment into the yellow box that appears.

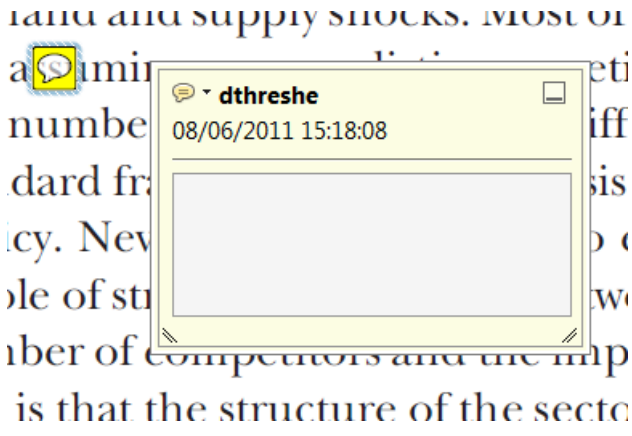

USING e-ANNOTATION TOOLS FOR ELECTRONIC PROOF CORRECTION

5. Attach File Tool – for inserting large amounts of text or replacement figures.

Inserts an icon linking to the attached file in the appropriate pace in the text.

How to use it

- Click on the Attach File icon in the Annotations section.
- Click on the proof to where you'd like the attached file to be linked.
- Select the file to be attached from your computer or network.
- Select the colour and type of icon that will appear in the proof. Click OK.

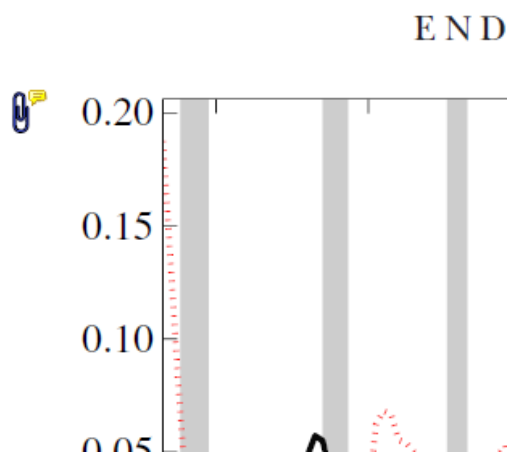

6. Add stamp Tool – for approving a proof if no corrections are required.

Inserts a selected stamp onto an appropriate place in the proof.

How to use it

- Click on the Add stamp icon in the Annotations section.
- Select the stamp you want to use. (The Approved stamp is usually available directly in the menu that appears).
- Click on the proof where you'd like the stamp to appear. (Where a proof is to be approved as it is, this would normally be on the first page).

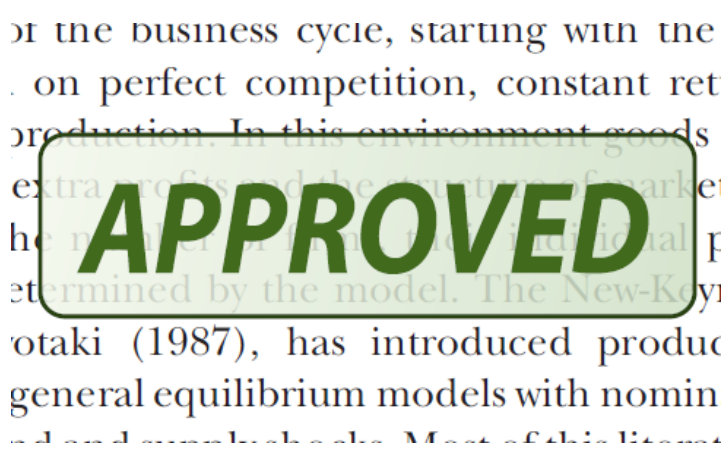

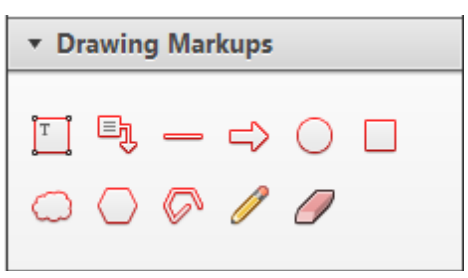

7. Drawing Markups Tools – for drawing shapes, lines and freeform annotations on proofs and commenting on these marks.

Allows shapes, lines and freeform annotations to be drawn on proofs and for comment to be made on these marks..

How to use it

- Click on one of the shapes in the Drawing Markups section.
- Click on the proof at the relevant point and draw the selected shape with the cursor.
- To add a comment to the drawn shape, move the cursor over the shape until an arrowhead appears.
- Double click on the shape and type any text in the red box that appears.

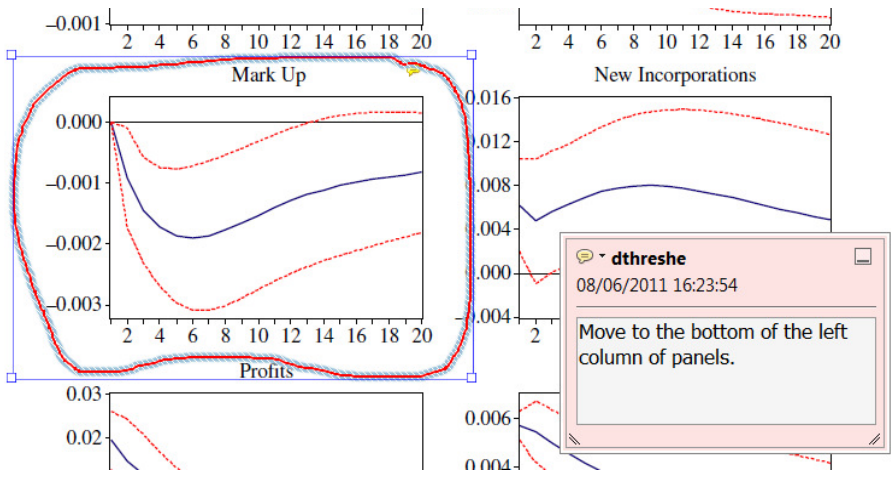

For further information on how to annotate proofs, click on the Help menu to reveal a list of further options: